INFLUENCE OF SAWDUST ASH AS A PARTIAL REPLACEMENT OF CEMENT IN CONCRETE

Abstract

The growing demand for sustainable construction materials has encouraged research into alternative binders and supplementary cementitious materials to partially replace cement in concrete. This study evaluates the mechanical, durability, and sustainability performance of concrete incorporating Sawdust Ash (SDA) as a partial replacement for cement, with replacement levels of 0%, 5%, 10%, and 15%. Experimental tests conducted included compressive strength, flexural strength, split tensile strength, and water permeability at 7, 14, 28, and 56 days. Results indicate distinct performance trends: while compressive strength decreased with SDA inclusion, the 10% replacement mix retained structural-grade strength (29.53 MPa at 28 days). Conversely, flexural strength improved significantly, peaking at 13.0 MPa with 10% SDA, outperforming the control mix.

Durability performance improved significantly with SDA incorporation, with water penetration depth reducing from 6.3 mm (control) to 5.5 mm (15% SDA), indicating enhanced pore refinement and pozzolanic densification. A sustainability assessment based on embodied carbon demonstrated progressive CO_2 reduction with increased SDA content, achieving up to 13.02% lower emissions at 15% replacement. Empirical regression modelling revealed a non-linear strength trend, confirming the experimental optimum. Overall, the study concludes that 10% SDA replacement offers the optimum balance of mechanical performance, durability, and sustainability benefits, making it a viable supplementary cementitious material for sustainable construction.

Keywords

Sawdust Ash (SDA), Partial Replacement, Compressive Strength, Flexural Strength, Durability, Water Permeability, Sustainability, Embodied Carbon, Empirical Modelling, Supplementary Cementitious Materials (SCMs).

1. Introduction

The construction industry plays a vital role in global economic development but faces increasing challenges related to the high cost, environmental impact, and sustainability of conventional building materials. Ordinary Portland Cement (OPC), the primary binder in concrete, is energy-intensive to produce and accounts for approximately 5–8% of global anthropogenic CO_2 emissions, with annual production exceeding 4.2 billion tonnes (Osanyinlokun et al., 2024; Meko and Ighalo, 2021). In developing countries such as Nigeria, the elevated cost of cement further hinders infrastructure development (Ikponmwosa et al., 2020). Additionally, the timber industry generates substantial waste, including over 1.8 million tons of sawdust annually in Nigeria alone, which, if unmanaged, contributes to landfill occupancy, environmental pollution, and harmful emissions when incinerated (Osanyinlokun et al., 2024; Mujedu et al., 2014; Chowdhury et al., 2015).

Sawdust ash (SDA), a pozzolanic by-product obtained from controlled incineration of sawdust, offers a promising supplementary cementitious material (SCM) for partial cement replacement. Its pozzolanic properties enable reaction with calcium hydroxide to form additional cementitious compounds, potentially reducing cement consumption, lowering costs, and promoting waste valorization while aligning with global sustainability goals (Meko and Ighalo, 2021; Marthong, 2012). Preliminary studies indicate that low to moderate SDA replacement levels (5–20%) can maintain or enhance concrete strength, but higher replacements often compromise performance due to reduced cement content, slower pozzolanic reactions, increased porosity, and diminished durability, particularly water permeability (Raheem et al., 2012; Mangi et al., 2017; Mujedu et al., 2014). However, comprehensive data on higher replacement levels (>10%), long-term durability, predictive performance models, and sustainability assessments remain limited and inconsistent, hindering widespread adoption of SDA as a reliable SCM (Ikponmwosa et al., 2020).

This knowledge gap underscores the need for systematic investigation into SDA-incorporated concrete. The present study addresses these limitations by examining the effects of SDA as a partial cement replacement on the fresh, mechanical, and durability properties of concrete. Specifically, it evaluates workability, compressive, split-tensile, and flexural strengths at various curing ages, water permeability, and overall performance compared to conventional OPC concrete across replacement levels of 0%, 5%, 10%, and 15%. Empirical models was developed using multivariate regression and interpolation techniques to predict performance trends, while a simplified embodied carbon assessment will quantify environmental benefits. These findings aim to establish the technical feasibility, optimal replacement threshold, and sustainability advantages of SDA as an economical, low-carbon alternative for structural and non-structural applications in concrete construction.

2. Materials and methods

2.1 Materials

Ordinary Portland cement (Dangote 3X, Type I) conforming to ASTM C150 was used, with physical properties including specific gravity of 3.1, density of 3.15 g/cm³, initial setting time of 71 min, and final setting time of 400 min. Fine aggregate was natural river sand passing 4.75 mm sieve, free of organic matter and salts (ASTM C33), with specific gravity 2.7, density 1.20 g/cm³, fineness modulus 3.03, and moisture content 1.21%. Coarse aggregate was crushed granite (maximum size 20 mm), angular, with specific gravity 2.65, density 1.5 g/cm³, moisture content 1.21%, absorption 0.35%, aggregate crushing value 17.76%, and impact value 7.43%. Sawdust ash (SDA) was prepared by air-drying sawdust, calcining at 600°C for 7 hours in a furnace, cooling, and sieving through 75 μm. XRF analysis showed major oxides: SiO_2 60.50%, CaO 11.55%, Al_2O_3 7.60%, with specific gravity 2.02 (Tables 3.4 and 3.5). SEM revealed surface morphology. Potable water meeting ASTM C1602 (pH ≥6.0) was used for mixing and curing.

2.2 Mix Design

Concrete mixes were designed using the DOE method for 30 MPa characteristic strength at 28 days, w/c ratio 0.48, and cement content ~469 kg/m³. SDA replaced cement at 0% (control), 5%, 10%, and 15% by weight. Aggregates were kept constant (fine: ~675 kg/m³; coarse: ~1011 kg/m³). Batch proportions per m³ and for specimens (cubes, beams, cylinders) are detailed in **Tables 1**. Replacement levels were selected based on literature (e.g., Marthong, 2012; Raheem et al., 2012) to balance pozzolanic benefits and performance.

Table 1: Concrete Mix Proportions (kg)

SDA Replacement (%)	W/C (kg/m³)	Cement	Fine Aggregate	SDA	Coarse Aggregate
0 (Control)	0.48	468.75	674.50	0	1011.75
5	0.48	445.31	674.50	23.44	1011.75
10	0.48	421.88	674.50	46.88	1011.75
15	0.48	398.44	674.50	70.31	1011.75
0 - (Control) 150 × 150 × 150 mm cube (per specimen)	0.7594	1.5820	2.2764	0	3.4147
5 - 150 × 150 × 150 mm cube (per specimen)	0.7594	1.5029	2.2764	0.0791	3.4147
10 - 150 × 150 × 150 mm cube (per specimen)	0.7594	1.4238	2.2764	0.1582	3.4147
15 - 150 × 150 × 150 mm cube (per specimen)	0.7594	1.3447	2.2764	0.2373	3.4147
0 (Control) - 100 × 100 × 400 mm beam (per specimen)	1.1250	2.3438	3.3725	0	5.0588
5 - 100 × 100 × 400 mm beam (per specimen)	1.1250	2.2266	3.3725	0.0791	5.0588
10 - 100 × 100 × 400 mm beam (per specimen)	1.1250	2.1094	3.3725	0.2344	5.0588
15 - 100 × 100 × 400 mm beam (per specimen)	1.1250	1.9922	3.3725	0.3516	5.0588
0 (Control) - 100 × 200 mm cylinder (per specimen)	0.3536	0.7366	1.0599	0	1.5899
5 - 100 × 200 mm cylinder (per specimen)	0.3536	0.6998	1.0599	0.0368	1.5899
10 - 100 × 200 mm cylinder (per specimen)	0.3536	0.6629	1.0599	0.0737	1.5899
15 - 100 × 200 mm cylinder (per specimen)	0.3536	0.6261	1.0599	0.1105	1.5899

2.3 Specimen Preparation and Curing

All materials were weighed using a digital scale. Mixing was done using a mechanical mixer until a uniform consistency was achieved. See figure 1 below

Figure 1: Batching of sand, cement and sawdust ash

The concrete was then placed into lubricated steel moulds and compacted in layers." Specimens were demoulded after 24 hours and "immersed in water at room temperature until the testing ages of 7, 14, 28, and 56 days." Specimen details are summarised in **Table 2**.

Table 2: Summary of Test Specimens

Property Tested	Specimen Type	Size (mm)	No.of Specimens per Mix	Test Ages
Compressive Strength	Beam	150 x 150 x 150	12	7,14, 28, 56
Split Tensile Strength	Cylinder	100 x 200	6	28, 56
Flexural Strength	Beam	100 x 100 x 400	6	28, 56
Water Permeability	Cube	150 x 150 x 150	6	56

2.4 Tests on Fresh Concrete

Workability was assessed via slump test (BS EN 12350-2) and compaction factor test (BS 1881: Part 103). Setting times of cement-SDA pastes were measured using Vicat apparatus (ASTM C191).

2.5 Tests on Hardened Concrete

Compressive strength was tested on 150 mm cubes (ASTM standards) at 7, 14, 28, and 56 days using

$$CTM: f_c = P/A.$$

Flexural strength on 100 × 100 × 400 mm beams (ASTM C293) at 28, 56 days: $\sigma = FL/wd^2$.

Split tensile strength on 100 × 200 mm cylinders at 28, 56 days:

$$f_t = 2P/\pi DL.$$

Water permeability on 150 mm cubes at 56 days (modified BS EN 12390-8): specimens subjected to 0.5–0.8 MPa water pressure for 72 hours, then split to measure penetration depth.

2.6 Empirical Modelling

Performance predictions used multivariate interpolation, multiple regression, and coefficient equations relating strength/permeability to SDA content and curing age.

2.7 Performance predictions used multivariate interpolation, multiple regression, and coefficient equations relating strength/permeability to SDA content and curing Sustainability Assessment

Embodied carbon (cradle-to-gate) was calculated per m³ using emission factors (e.g., cement 0.85–0.95 kg CO_2/kg; SDA 0.05–0.15 kg CO_2/kg) from ICE v3.0 and literature:

$$EC_{mix} = \sum(W_i \times EF_i)$$

where:

W_i= mass of each material in kg,

EF_i = emission factor (kg CO_2/kg).

Table 3: Embodied Carbon Factors

Material	Emission factor (kg co_2 / kg)	Source
Cement	0.85 – 0.95	ICE v3.0 / GNR
Fine aggregate	0.005 – 0.010	ICE v3.0
Coarse aggregate	0.005 – 0.010	ICE v3.0
Sawdust ash (SDA)	0.05 – 0.15	Literature (calcination energy)
Water	0.0003	ICE v3.0

3. Results and Discussions

Table 4: Fine Aggregate Characterization

Sieve Size	Mass Retained (g)	Cumulative Mass Retained (g)	Cumulative Retained (%)	Cumulative Passing (%)
4.75	10.11	10.11	2.022	97.978
2	51.71	61.82	12.364	87.636
0.85	147.31	209.13	41.826	58.174
0.425	123.91	333. 04	66.608	33.392
0.212	86.01	419.05	83.81	16.19
0.15	40.21	459.26	91.852	8.148
0.075	34.41	493.67	98.734	1.266
Pan	6.33	500.00	100	0

Figure 2: Particle Size Distribution Curve (Fine Aggregate)

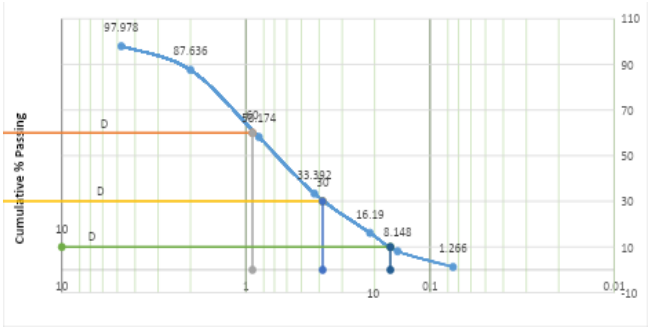

The sieve analysis of the fine aggregate yielded a uniformity coefficient (Cu) of 5.6080, calculated as D60/D10, and a coefficient of curvature (Cc) of 0.9692, determined from $(D30)^2/(D10 \times D60)$. The fineness modulus was found to be 3.03.

For bulk density determination, an empty beaker weighed 120.2 g. After adding the fine aggregate sample, the total weight was 904.2 g, giving a sample weight of 784 g (904.2 g – 120.2 g). The beaker, used as a cylinder, had a height of 10.8 cm and a diameter of 8.8 cm, resulting in a volume of 656.87 cm³ (calculated as $\pi \times (4.4)^2 \times 10.8$, with π approximated as 22/7). The bulk density was therefore 784 g / 656.87 cm³ = 1.19 g/cm³.

The specific gravity of the fine aggregate was determined using a pycnometer. The mass of the empty pycnometer (M1) was 148.1 g, the pycnometer filled with sample (M2) was 210.0 g, the pycnometer with sample and water (M3) was 298.7 g, and the pycnometer filled with water only (M4) was 259.6 g. The specific gravity (Gs) was calculated as (M2 – M1) / [(M2 – M1) – (M3 – M4)] = 2.7.

Table 5: Coarse Aggregate Characterization

Sieve Size	Mass Retained (g)	Cumulative Mass Retained (g)	Cumulative Retained (%)	Cumulative Passing (%)
25	22.5	22.5	4.5	95.5
19	332.2	354.7	70.94	29.06
9.5	141.2	495.9	99.18	0.82
4.75	1.9	497.8	99.56	0.44
Pan	2.2	500	100	0

Figure 3: Particle Size Distribution Curve (Coarse Aggregate)

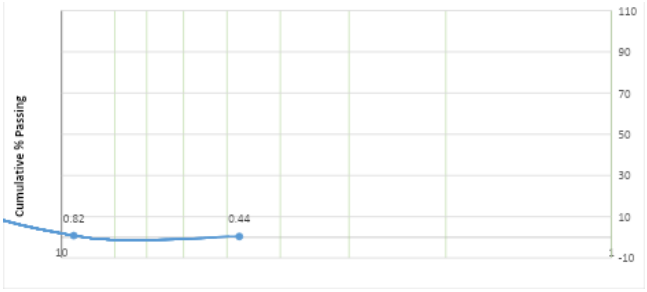

The specific gravity and water absorption of the coarse aggregate were determined as follows: the submerged weight was 740.9 g, the saturated surface dry (SSD) weight was 1189.2 g, and the oven-dry weight was 1185.1 g. Water absorption was calculated as [(SSD – Dry)/Dry] × 100 = 0.346%. The specific gravity was computed as SSD/(SSD – Submerged) = 2.65.

For bulk density, the mass of coarse aggregate in the cylindrical container was 2737.4 g (2.7374 kg). The container had a height of 17.8 cm (0.178 m) and a diameter of 11.3 cm (0.113 m), giving a volume of 1.7851×10^{-3} m³. The bulk density was therefore mass/volume = 1533.46 kg/m³.

The aggregate crushing value (ACV) test yielded the following: mass of sample (A) = 2737.4 g; mass after crushing and sieving (B) = 2251.2 g; mass passing 2.36 mm sieve (A – B) = 486.2 g. The ACV was calculated as [(A – B)/A] × 100 = 17.76%.

The aggregate impact value (AIV) test results were: mass of sample (A) = 363.5 g; mass after impact and sieving (B) = 336.5 g; mass passing 2.36 mm sieve (A – B) = 27 g. The AIV was calculated as [(A – B)/A] × 100 = 7.43%.

3.1 Physical and Chemical Properties of Materials

3.1.1 Physical Properties

The physical properties of the primary materials are summarised in **Table 6**. Sawdust ash (SDA) displayed lower specific gravity (2.23) and bulk density (870 kg/m³) than cement (3.14 and 1440 kg/m³, respectively), consistent with the lighter nature of ash-based pozzolans (Raheem et al., 2012). The finer particles of SDA (fineness modulus 5.4) contribute to improved particle packing and filling effect, enhancing strength at lower replacement levels.

Table 6: Physical Properties of Materials

Property	Cement	SDA	Fine Aggregate	Coarse Aggregates
Specific Gravity	3.14	2.23	2.7	2.64
Bulk Density	1440	870	1190	1533
Fineness Modulus	8.2	5.4	3.03	------
Colour	Grey	Light Grey	Brownish	Dark Grey

3.1.2 Chemical Composition of Sawdust Ash

The oxide composition of SDA, determined by XRF analysis, is presented in **Table 7**. The combined SiO_2 + Al_2O_3 + Fe_2O_3 content was 70.70%, satisfying the ASTM C618 requirement (>70%) for Class F pozzolans and confirming strong pozzolanic potential. Moderate CaO (3.10%) supports later-age strength gain, while low loss on ignition (LOI = 2.65%) indicates effective calcination and minimal unburnt carbon.

Table 7: Chemical Composition of Sawdust Ash

Oxide	Composition(%)
SiO_2	60.50
Al_2O_3	7.60
Fe_2O_3	2.60
CaO	3.10
MgO	1.25
SO_3	3.10
LOI	2.65

3.2 Fresh Properties of SDA-Concrete

3.2.1 Workability (Slump Test)

Slump values decreased progressively with increasing SDA replacement (Table 8), from 90 mm (control) to 65 mm at 15% SDA. This reduction is attributed to the higher surface area and porous structure of SDA, which increases water demand. Nevertheless, slump remained within acceptable ranges for normal concrete, particularly at ≤10% replacement, suggesting no need for additional water or admixtures at moderate levels.

Table 8: **Slump Test Results**

Mix ID	SDA(%)	Slump (mm)
M_0	0	90
M_1	5	85
M_2	10	78
M_4	15	65

3.2.2 Setting Time and Compaction Factor

Incorporation of SDA slightly prolonged initial and final setting times due to dilution of cement and slower pozzolanic reaction. Compaction factor also declined with higher SDA content, further indicating reduced workability.

3.2.3 Density of Hardened Concrete

Hardened density decreased with rising SDA content, reflecting the lower specific gravity of SDA compared to cement. This trend supports the potential development of lightweight structural concrete, in agreement with findings reported by Ikponmwosa et al. (2020).

Figure 4: Variation of Slump with SDA

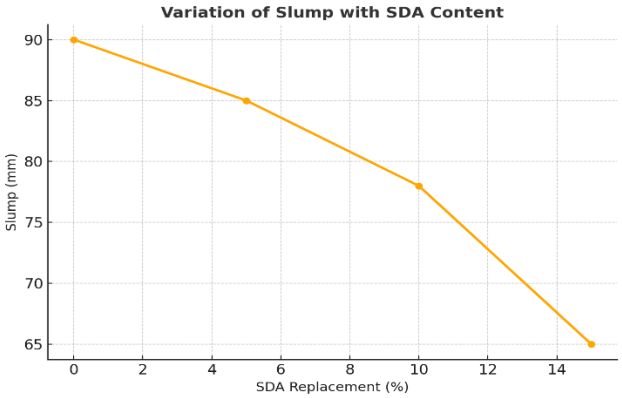

3.3 Mechanical Properties of SDA-Concrete

3.3.1 Compressive Strength

Compressive strength results at 7, 14, 28, and 56 days are presented in Table 9. Strength increased with curing age for all mixes, with the control (0% SDA) achieving the highest values, peaking at 38–41 MPa at 56 days. Partial replacement with SDA reduced strength progressively: 5% SDA retained reasonable performance (30.9 MPa at 28 and 56 days), while 10% and 15% showed marked declines, particularly beyond 28 days (22.56 MPa and 12.7 MPa at 56 days, respectively). The reduction at higher replacements is attributed to cement dilution and slower pozzolanic reaction. Optimal performance was observed at 5–10% SDA, consistent with previous studies (Marthong, 2012; Raheem et al., 2012).

Table 9: Compressive Strength (MPa)

SDA (%)	7 Days	14 Days	28 Days	56 Days
0	31.9	34.0	35.83	38.0
5	25.0	31.5	30.9	30.9
10	20.4	25.1	29.53	22.56
15	16.7	19.6	21.6	12.7

3.3.2 Split Tensile Strength

Split tensile strength at 28 and 56 days (Table 10) exhibited a slight enhancement at 5% SDA (3.5 MPa at 28 days vs. 3.3 MPa control), followed by declines at higher replacements (3.2 MPa at 10%; 2.4 MPa at 15% at 28 days). At 56 days, values converged lower than the control (3.8 MPa), with 5–15% SDA ranging 2.9–3.4 MPa. The initial improvement at low replacement is linked to filler effects and pore refinement in the interfacial transition zone (ITZ), while higher SDA contents impair matrix continuity and tensile capacity (Awoyera & Adesina, 2020; Cordeiro et al., 2009; Chusilp et al., 2009).

Table 10: Split Tensile Strength (MPa)

SDA (%)	28 Days	56 Days
0	3.3	3.8
5	3.5	3.4
10	3.2	3.0
15	2.4	2.9

3.3.3 Flexural Strength

Flexural strength (Table 11) showed a distinct trend, with 10% SDA outperforming the control at 28 days (13.0 MPa vs. 10.3 MPa), likely due to enhanced microfiller packing and ITZ bonding. At 5% SDA, values were lower (8.9 MPa), and 15% SDA yielded 11.4 MPa. By 56 days, the control reached 17.6 MPa, while SDA mixes converged at 13.0–13.3 MPa. Long-term pozzolanic activity partially compensated for cement reduction, but flexural strength remained below control at higher replacements. Overall, 10% SDA provided optimal bending performance, benefiting more from microstructural densification than tensile or compressive strength (Neville, 2011; Bheel et al., 2018; Adesanya & Raheem, 2009).

Table 11: Flexural Strength (MPa)

SDA (%)	28 Days	56 Days
0	10.3	17.6
5	8.9	13.3
10	13.0	13.0
15	11.4	13.3

3.4 Durability Properties

3.4.1 Water Permeability

Water penetration depth at 56 days under 0.5 MPa pressure decreased with SDA incorporation (Table 12), from 6.3 mm (control) to 5.5 mm at 15% SDA. Optimal reduction occurred at 10–15% (5.9–5.5 mm), attributed to pozzolanic formation of additional C–S–H gel, pore refinement, and ITZ densification. All mixes exhibited low permeability (<15 mm), indicating favourable resistance to water ingress per BS EN 12390-8 (Awoyera & Adesina, 2020; Cordeiro et al., 2009; Mehta & Monteiro, 2014).

Table 12: Depth of Water Penetration at 56 Days

SDA (%)	Penetration Depth (mm)	Pressure (MPa)
0	6.3	0.5
5	6.1	0.5
10	5.9	0.5
15	5.5	0.5

3.5 Empirical Model Development

Slump decreased with increasing SDA content (Table 13), confirming reduced workability at higher replacements. Compressive strength statistics across all ages and mixes: minimum 11.3 MPa, maximum 41.0 MPa, mean 26.65 MPa. Strength at 5–10% SDA remained comparable to control, while 15% showed consistent reductions.

Table 13: Mean Slump Values

SDA (%)	Mean Slump (mm)
0	90–95
5	80–85
10	75–80
15	65–70

Figure 5: Box Plots of strength distribution

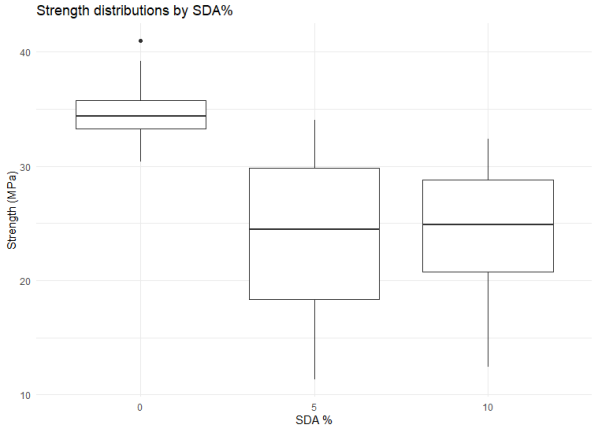

3.5.1 Multivariate Surface Interpolation

Multivariate interpolation using the Akima algorithm generated a continuous 3D surface relating compressive strength to SDA replacement level and curing age (Figure 6). The surface revealed that strength consistently increased with age across all SDA contents. Maximum strength occurred along a

ridge corresponding to 5–10% SDA, beyond which the surface declined sharply, particularly at later ages. This pattern aligns with the pozzolanic contribution of SDA being most effective at moderate replacement levels.

Figure 6: 3D surface: Strength (SDA, Day)

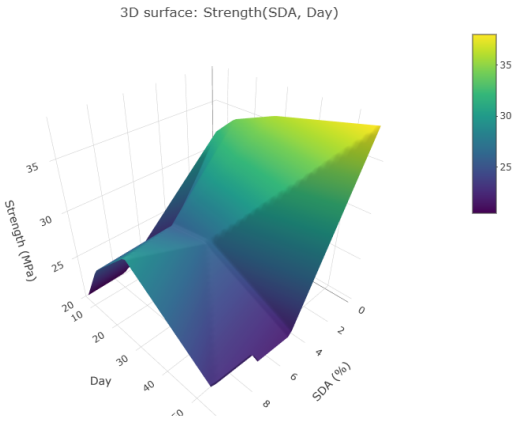

3.5.2 Multiple Regression Analysis

Two multiple regression models were developed to predict compressive strength (Table 14).

Linear interaction model:

$$f_c = 29.907 - 0.787(\text{SDA}) + 0.076(\text{Day}) - 0.010(\text{SDA} \times \text{Day})$$

($R^2 = 0.251$, Adjusted $R^2 = 0.199$),

indicating limited linear predictive power.

Quadratic model (superior fit): Included a significant SDA^2 term (-3.21 for SDA linear, +0.243 for SDA^2; both $p < 0.01$), yielding $R^2 = 0.410$, Adjusted $R^2 = 0.355$, and lower AIC (317.65). The positive quadratic coefficient confirms non-linear behaviour with peak strength at intermediate SDA levels (~10%).

Table 14: Multiple Regression Coefficients for Compressive Strength

Model	Term	Estimate	p-value	Model Performance
Linear	Intercept	29.907	<0.001	$R^2 = 0.251$ Adj. $R^2 = 0.199$
	SDA	–0.787	0.110	
	Day	0.076	0.411	
	SDA × Day	–0.010	0.505	
Quadratic	SDA	–3.21	0.00038	$R^2 = 0.410$ Adj. $R^2 = 0.355$ AIC = 317.65
	SDA^2	0.243	0.00145	

3.5.3 Model Diagnostics and Validation

Diagnostic plots (Figures 7–12) showed random residual scatter with minor tail deviations from normality and mild heteroskedasticity (Breusch–Pagan $p = 0.056$). Durbin–Watson statistic (0.74, $p < 0.0001$) indicated positive autocorrelation, likely due to repeated measures. Five-fold cross-validation yielded RMSE = 7.20 MPa and $R^2 = 0.17$, demonstrating acceptable predictive performance given inherent variability in concrete strength data.

fig 7-12-- Diagnostic plots showing random residual scatter with minor tail deviations from normality and mild heteroskedasticity

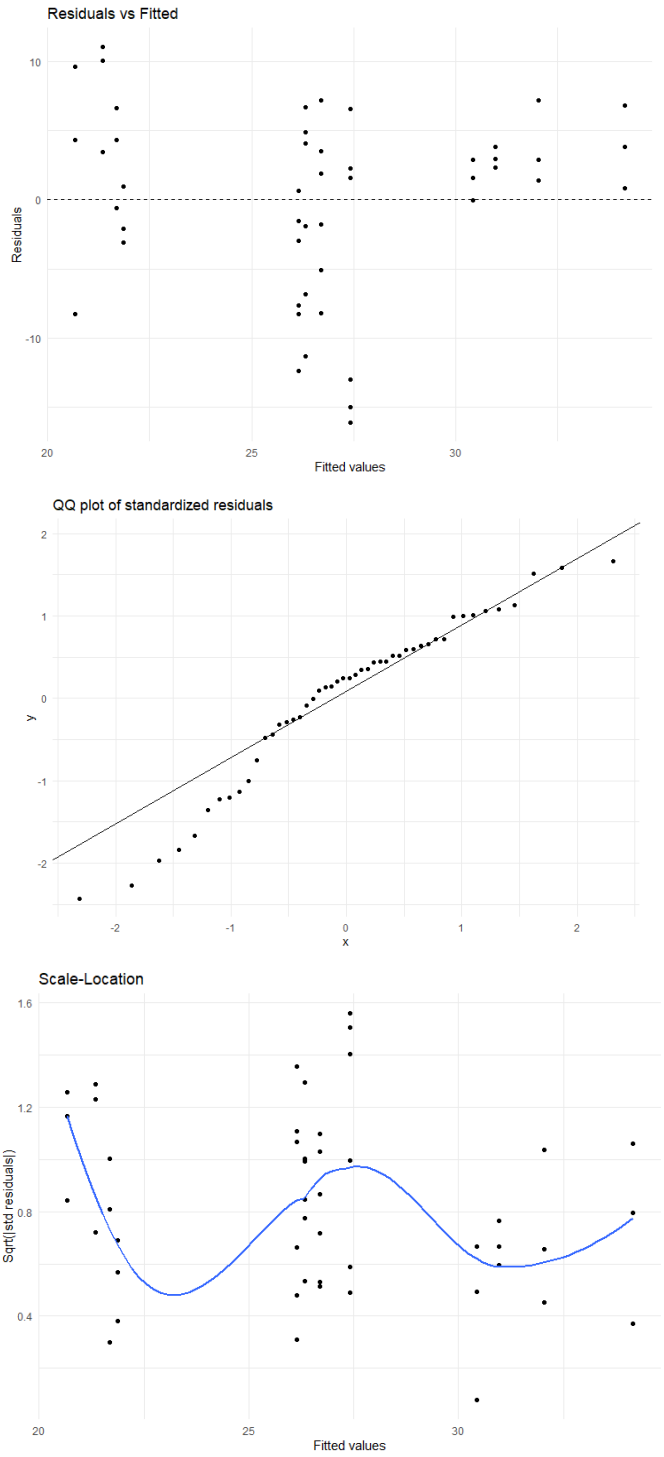

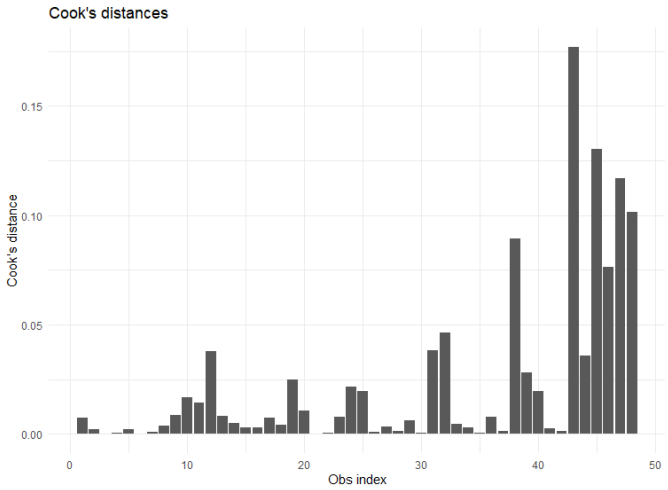

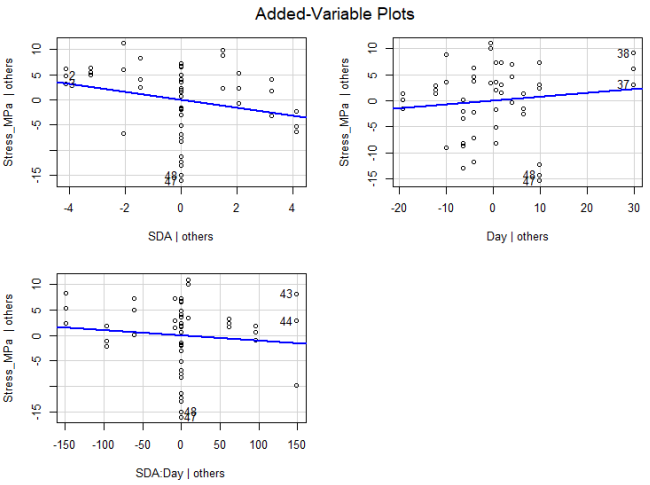

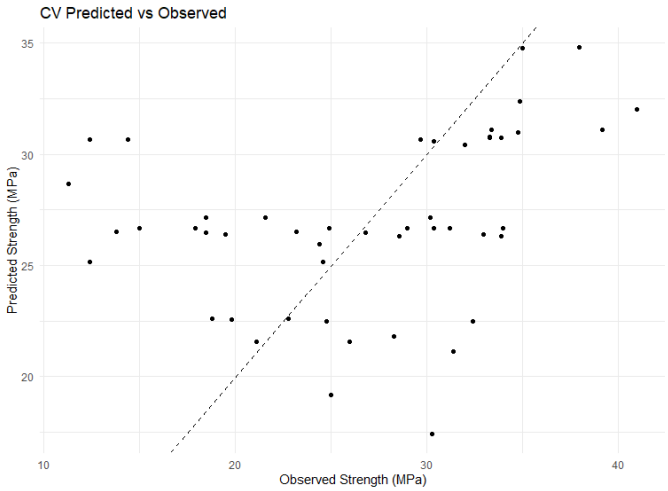

3.5.4 Empirical Coefficient Equation for Compressive Strength

The quadratic regression model yielded an empirical equation for predicting **compressive strength** (MPa) within the tested ranges (SDA 0–15%; curing age 7–56 days).

$$f_c = 29.907 - 0.787(SDA) + 0.076(Day) - 0.01004(SDA \cdot Day)$$

Example prediction: At 5% SDA and 28 days, the model aligns closely with observed values.

$$f_c = 26.69 \text{ MPa}$$

3.5.5 Flexural Strength Analysis

Regression analysis for flexural strength produced $R^2 = 0.74$ (Adjusted $R^2 = 0.545$). Curing age was significant ($p = 0.035$), with SDA exerting moderate influence (Figure 4.13). Flexural strength increased with age, peaking around 10% SDA due to an interaction term indicating diminishing returns at higher replacements.

Figure 13: Graph of Flexural Strength vs SDA

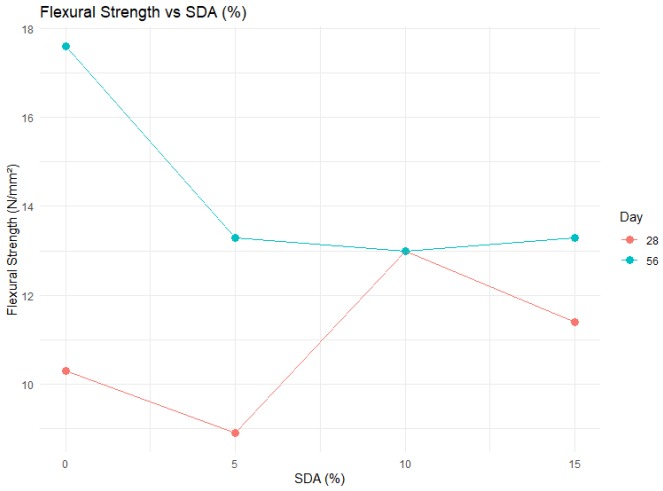

3.5.6 Split Tensile Strength Analysis

The model for split tensile strength showed $R^2 = 0.782$ (Adjusted $R^2 = 0.618$), with only the intercept significant (Figure 14). SDA caused a slight overall reduction, modest up to 10% but more pronounced at 15%.

Figure 14: Scatter plots of split tensile strength

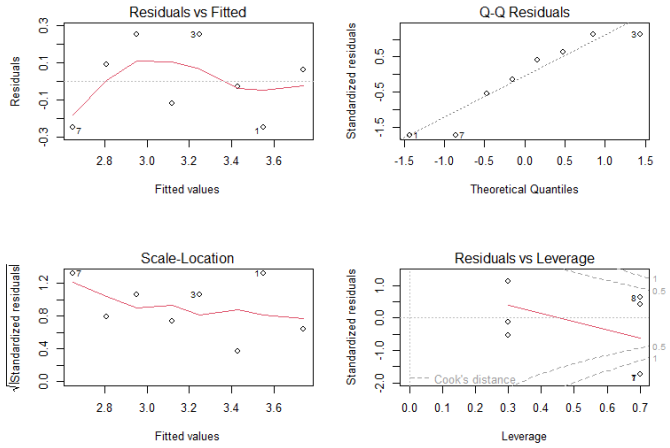

3.5.7 Water Permeability Analysis

Regression for 56-day water penetration depth yielded a strong linear fit ($R^2 = 0.966$, Adjusted $R^2 = 0.949$; $p = 0.017$) (Figure 15). Permeability decreased with higher SDA content, reflecting enhanced microstructural densification via pozzolanic reaction.

Figure 15: Scatter plots of water permeability

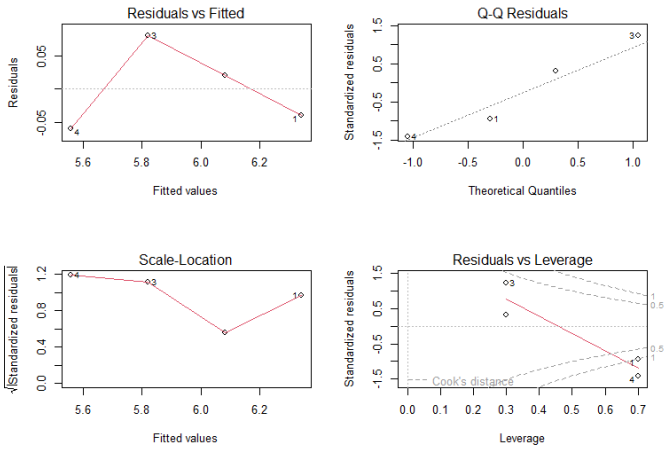

3.5.8 Comparative Analysis of Mechanical Properties

At 28 days (Figure 16), compressive and flexural strengths peaked at 10% SDA, while split tensile strength remained stable or slightly enhanced up to 5–10% before declining. Overall summary (Table 15): 10% SDA provided optimal mechanical performance, whereas 15% maximised durability (lowest permeability).

Figure 16: Graph of mechanical property comparison at 28 days

Table 15: Overall Performance Summary

Property	**Control**	**5% SDA**	**10% SDA**	**15% SDA**	**Best**
Compressive	High	Slightly ↓	**Peak**	Reduced	**10%**
Flexural	Moderate	↓	**Peak**	↓	**10%**
Tensile	Stable	~Equal	Slight ↓	Significant ↓	**5–10%**
Permeability	High	↓	↓↓	↓↓↓	**15%**

Conclusion

According to the statistical analysis and experimental results the following findings are taken:

i. The employed Sawdust Ash serves as a good supplementary cementitious material (SCM) with high silica content (60.50%) and is active in C-S-H gel formation in the secondary stage, as it can actively produce its secondary C-S-H gel, especially at later curing ages (28–56 days).

ii. Incorporation of SDA reduces the workability of the new concrete, as the new solution has a relatively high specific surface area and requires a greater volume of water. Slump levels decreased from 90 mm (Control) to 65 mm (15% SDA), while cohesion and structural workability of the mix was maintained.

iii. The replacement with 10% SDA is the structural optimum, with a 28-day strength of 29.53 MPa. This is above a minimum requirement of concrete strength (25 MPa) used in structural concrete, whereas 15% SDA produced a significant drop in strength (21.6 MPa). With SDA inclusion, the flexural performance performed better, with a maximum of 13.0 MPa for the 10% mix at 28 days and 10.3 MPa for the control. This reflects improved interfacial bond strength and pore refinement.

iv. SDA improves water tightness of concrete significantly. Water penetration depth decreased from 6.3 mm (Control) to 5.5 mm (15% SDA) at 56 days. This corroborates that SDA is an efficient micro-filler as it fine-tunes the pore architecture, and decreases the permeability.

v. Partially replacing cement with SDA has linear environmental benefits. The maximum embodied carbon reduction was achieved by 15% SDA blend, reducing CO_2 emissions by 13.02% (from 443.12 kg CO_2/m^3 to 385.46 kg CO_2/m^3).

vi. The relationship between SDA content and compressive strength is nonlinear and quadratic. The applied empirical regression model developed ($R^2 = 0.41$) indicates that strength reaches a maximum between 5% and 10% before decreasing, as suggested by the experimental results.

Recommendation

Sawdust ash can be effectively incorporated as a partial cement replacement in concrete production. For structural applications, replacement levels of 5–10% are recommended, as they maintain or enhance mechanical performance without significant compromise; specifically, 10% SDA is ideal for general reinforced concrete elements requiring a balance of strength and durability, whereas 15% may be suitable for non-structural or low-load applications where enhanced impermeability is the priority. In projects aimed at minimising environmental impact, 10–15% SDA should be adopted to achieve the greatest reductions in embodied carbon.

Further research is advised to optimise SDA through finer grinding, adjusted calcination conditions, or chemical activation, potentially extending the viable replacement range. Long-term durability evaluations, including chloride diffusion, carbonation depth, and sulfate resistance, are essential to confirm real-world performance. The empirical equations derived in this study should be utilised for predicting strength within the tested parameters (0–15% SDA and 7–56 days curing). Future modelling efforts could incorporate additional factors such as curing temperature, admixtures, and exposure conditions to improve predictive accuracy.

References

Abdullahi, A., Abubakar, M. and Afolayan, A. 2013. Partial replacement of sand with sawdust in concrete production. 3rd Biennial Engineering Conference. Federal University of Technology, Minna. 1–6.

Abed, J. M. and Khaleel, B. A. 2019. Effect of wood waste as a partial replacement of cement, fine and coarse aggregate on physical and mechanical properties of concrete blocks units. International Journal of Integrated Engineering 11.8: 229–239.

Adesanya, D. A. and Raheem, A. A. 2009a. A study of the workability and compressive strength characteristics of corn cob ash blended cement concrete. Construction and Building Materials 23.1: 311–317.

Adesanya, D. A. and Raheem, A. A. 2009b. Development of corn cob ash blended cement. Construction and Building Materials 23: 347–352.

Adesanya, D. A. and Raheem, A. A. 2010. A study of the permeability and acid attack of corn cob ash blended cements. Construction and Building Materials 24: 403–409.

Adewuyi, A. and Adegoke, T. 2008. Optimization of waste sawdust ash as partial replacement for cement. Journal of Engineering Research.

Akinwumi, I. I., Olatunbosun, B. J. and Olofinnade, O. M. 2015. Soil stabilization using sawdust ash. Journal of Applied Sciences and Environmental Management 19.2: 259–266.

Assiamah, S., Kankam, C.K., Adinkrah-Appiah, K. 2025. The impact of burnt sawdust ash from timber species as partial cement replacements on the durability properties for sustainable interlocking blocks. Discov Civ Eng 2, 20 https://doi.org/10.1007/s44290-025-00183-2

Assiamah, S., Agyeman, S., Adinkrah-Appiah, K. and Danso, H. 2022. Utilization of sawdust ash as cement replacement for landcrete interlocking blocks production and mortarless construction. Case Studies in Construction Materials 16: e00945.

Auta, S. M., Uthman, A., Sadiku, S. and Shiwua, A. J. 2016. Flexural strength of reinforced revibrated concrete beam with sawdust ash as a partial replacement for cement. Construction of Unique Buildings and Structures 5.44: 31–45.

Awoyera, P. O. and Adesina, A. 2020. A review on the mechanical properties of cement-based composites reinforced with industrial and agricultural wastes. Journal of Building Engineering 31: 101295.

Ayuba, S., Uche, O., Haruna, S. and Mohammed, A. 2022. Durability properties of cement–sawdust ash (SDA) blended self-compacting concrete (SCC). Balendran, R. V. and Martin-Buades, W. H. 2000. The influence of high temperature curing on the compressive, tensile and flexural strength of pulverized fuel ash concrete. Building and Environment 35.5: 415–423.

Bheel, N., Abbasi, S. A., Memon, S. A. and Khahro, S. H. 2018. Effects of supplementary cementitious materials on permeability and durability properties of concrete. International Journal of Advanced Materials Science 9.1: 1–13.

Bheel, N., Abbasi, S. A., Memon, S. A. and Khahro, S. H. 2018. Mechanical performance of concrete incorporating waste materials. International Journal of Advanced Materials Science 9.1: 1–13.

British Standard Institution. 1976. BS 5224: Standard specification for masonry cement. London: BSI.

British Standard Institution. 1978. BS 12: Ordinary and rapid hardening Portland cement. London: BSI.

British Standard Institution. 1983. BS 1881: Part 102: Methods for determination of slump. London: BSI.

British Standard Institution. 1983. BS 1881: Part 116: Methods for determination of compressive strength of concrete cubes. London: BSI.

British Standard Institution. 1985. BS 8110: Structural use of concrete: code of practice for design and construction. London: BSI.

BS EN 12390-8. 2019. Testing hardened concrete – Part 8: Depth of penetration of water under pressure. European Committee for Standardization.

Cheah, C. B. and Ramli, M. 2011. The implementation of wood waste ash as a partial cement replacement material in the production of structural grade concrete and mortar: an overview review article. Resources, Conservation and Recycling 55.1: 669–685.

Cheng, Y., Liu, J., Wang, W., Jin, L. and Yan, S. 2024. Preparation and property study of sawdust-modified cement mortar. Frontiers in Materials.

Chowdhury, S., Maniar, A. and Suganya, O. 2014. Strength development in concrete with wood ash blended cement. International Journal of Sustainable Built Environment 3.2: 86–92.

Chowdhury, S., Mishra, M. and Suganya, O. 2015. The incorporation of wood waste ash as a partial cement replacement material for making structural grade concrete: an overview. Ain Shams Engineering Journal 6.2: 429–437.

Chusilp, N., Jaturapitakkul, C. and Kiattikomol, K. 2009. Effects of ash fineness and replacement level of rice husk ash on compressive strength and water permeability of controlled low-strength materials. Construction and Building Materials 23.1: 214–220.

Cordeiro, G. C., Toledo Filho, R. D. and Fairbairn, E. M. 2009. Use of ultrafine ash from sugarcane bagasse combustion as mineral admixture in concrete. ACI Materials Journal 106.1: 81–87.

Dulipalla, S. 2018. Study on partial replacement of cement by saw dust ash in concrete. International Journal for Research in Applied Science and Engineering Technology 6.2: 747–752.

Ecoinvent Centre. 2021. Ecoinvent database v3.7. Swiss Centre for Life Cycle Inventories.

Elinwa, A. U. and Mahmood, Y. A. 2002. Ash from timber waste as cement replacement material. Cement Concrete Composites 24: 219–222.

Elinwa, A. U., Ejeh, S. P. and Mamuda, A. M. 2008. Assessing of the fresh concrete properties of self-compacting concrete containing sawdust ash. Construction and Building Materials 22.6.

EN 15804. 2019. Sustainability of construction works – environmental product declarations. European Committee for Standardization.

Folagbade, S. O. and Aluko, O. G. 2019. Permeation resistance of sawdust ash blended cement laterized concrete. Civil Engineering Dimension 21.2: 76–83.

Food and Agricultural Organization (FAO) Records. 2002. Retrieved from http://apps.fao.org/default.htm.

Gambhir, M. L. 2004. Concrete technology. New Delhi: Tata McGraw – Hill Publishing Company Limited. 352-448.

Gwarah, L. S., Akatah, B. M., Onungwe, I. and Akpan, P. P. 2019. Partial replacement of ordinary Portland cement with sawdust ash in concrete. Current Journal of Applied Science and Technology 32.6: 1–7.

Hague, M. N. and Kayali, O. 1998. Properties of high strength concrete using a fine fly ash. Cement and Concrete.

Hammond, G. and Jones, C. 2011. Inventory of carbon and energy (ICE). Version 3.0. UK: University of Bath.

Hossain, K. M. A. 2005. Blended cement using volcanic ash and pumice. Cement and Concrete Research 33: 1601–1605.

IITA. 2002. Maize. Retrieved from http://intranet/iita4/crop/maize.htm.
Ikponmwosa, E. E., Falade, F. A., Fashanu, T., Ehikhuenmen, S. and Adesina, A. 2020. Experimental and numerical investigation of the effect of sawdust ash on the performance of concrete. Journal of Building Pathology and Rehabilitation 5.1.

Islam, M. S., Rahman, M. M. and Ahmed, M. 2011. Properties of concrete using rice husk ash. Journal of Civil Engineering (IEB) 39.1: 37–44.

Kolawole, J. O. and Mbachu, J. I. C. 1998. Shrinkage and elastic moduli of ordinary Portland cement (OPC) and rice husk ash (RHA) concrete made with difference coarse aggregate types. Journal of Environmental Science 1.2: 35–40.

Kryton. 2024. Durability testing 101: the water permeability test. Kryton International Blog. Retrieved from https://www.krystol.co.nz/blog/post/125613/durability-testing-101-the-water-permeability-test/.

Kumar, R. V. and Krishna, M. S. R. 2016. A case study on partial replacement of cement by saw dust ash in concrete. International Journal of Science and Research 5.6: 275–280.

Majeed, S. S. 2024. Formulating eco-friendly foamed mortar by incorporating sawdust ash as a partial cement replacement. Sustainability 16.7: 2612.

Mangi, S. A., Jamaluddin, N., Wan, I. M. H., Mohamad, N. and Sohu, S. 2017. Utilization of sawdust ash as cement replacement for the concrete production: a review. Engineering Science and Technology International Research Journal 1.3: 11–15.

Marthong, C. 2012. Sawdust ash (SDA) as partial replacement of cement. International Journal of Engineering Research and Applications 2.4: 1980–1985.

Meddah, S. 2017. Recycled aggregates in concrete production: engineering properties and environmental impact. MATEC Web of Conferences 101: 05021.

Mehta, P. K. and Monteiro, P. J. M. 2014. Concrete: microstructure, properties and materials. 4th ed. McGraw-Hill.

Meko, B. and Ighalo, J. O. 2021. Utilization of Cordia africana wood sawdust ash as partial cement replacement in C 25 concrete. Cleaner Materials 1: 100012.

Muhedin, D. A., Qadir, S. J., Hamakareem, M. I. and Rash, A. J. H. 2020. Effect of sawdust as partial replacement of sand in concrete. Journal of University of Duhok 23.2: 658–664.

Mujedu, K. A., Adebara, S. A. and Lamidi, I. O. 2014. The use of corn cob ash and saw dust ash as cement replacement in concrete works. The International Journal of Engineering and Science 3.4: 22–28.

Neville, A. M. 2011. Properties of concrete. 5th ed. Pearson Education.

Ogork, E.-N. N. and Ayuba, S. 2014. Influence of sawdust ash (SDA) as admixture in cement paste and concrete. International Journal of Innovative Science, Engineering & Technology 1.10: 736–743.

Olafusi, O. S. and Olutoge, F. A. 2012. Strength properties of corn cob ash concrete. A Journal of Emerging Trends in Engineering and Applied Sciences 3.2: 297–301.

Olu, O. O. 2020. Effect of saw dust ash and eggshell powder on the properties of cement blends. American Journal of Construction and Building Materials 4.2: 88–99.

Olutoge, F. A., Bhashya, V., Bharatkumar, B. H. and Sundar, K. S. 2010. Comparative studies on fly ash and GGBS high performance concrete. Proceeding of National Conference on Recent Trend and Advance in Civil Engineering – TRACE 2010.

Omar, M. F., Abdullah, M. A. H., Rashid, N. A. and Abdul Rani, A. L. 2020. Partially replacement of cement by sawdust and fly ash in lightweight foam concrete. IOP Conference Series: Materials Science and Engineering 743.1: 012035.

Osanyinlokun, O. E., Fapohunda, C. A. and Olaniyan, O. M. 2024. Compressive, bending and shear properties of reinforced concrete beams containing sawdust ash as partial replacement of cement. Nigerian Journal of Technology 43.1: 2–13.

Osuya, D. O. and Mohammed, H. 2017. Evaluation of sawdust ash as a partial replacement for mineral filler in asphaltic concrete. Ife Journal of Science 19.2: 431–440.

Oyedepo, O. J., Oluwajana, S. D. and Akande, S. P. 2014. Investigation of properties of concrete using sawdust as partial replacement for sand. Civil and Environmental Research 6.2.

Oyekan, G. L. and Kamiyo, O. M. 2011. A study on the engineering properties of sandcrete blocks produced with rice husk ash blended cement. Journal of Engineering and Technology Research 3.3: 88–98.

Raheem, A. A. and Adesanya, D. A. 2011. A study of thermal conductivity of corn cob ash blended cement mortar. The Pacific Journal of Science and Technology 12.2: 106–111.

Raheem, A. A. and Sulaiman, O. K. 2013. Saw dust ash as partial replacement for cement in the production of sandcrete hollow blocks. International Journal of Engineering Research and Applications 3.4: 713–721.

Raheem, A. A., Falola, O. O. and Adeyeye, K. J. 2012a. Production and testing of lateritic interlocking blocks. Journal of Construction in Developing Countries, Malaysia 17.1: 35–50.

Raheem, A. A., Olasunkanmi, B. S. and Folorunso, C. S. 2012b. Saw dust ash as partial replacement for cement in concrete. Organization, Technology and Management in Construction: An International Journal 4.2: 474–480.

Raheem, A. A., Oyebisi, S. O., Akintayo, S. O. and Oyeniran, M. I. 2010. Effects of admixtures on the properties of corn cob ash cement concrete. Leonardo Electronic Journal of Practices and Technologies 16: 13–20.

Sawant, A., Sharm, A., Rahate, R., Mayekar, N. and Ghadge, M. D. 2018. Partial replacement of sand with sawdust in concrete. International Research Journal of Engineering and Technology 5.3: 3098–3101.

Siddique, R. 2008. Utilization of sawdust ash in concrete. Resources, Conservation and Recycling 52.1: 1–13.

Singh, Er. N. and Singh, H. 2022. A study on the strength of concrete by partial cement replacement with sawdust ash. Ymer 21.8: 699–715.

Ugboaja, C. E., Ezeagu, C. A., Okonkwo, V. O. and Agbo-Anike, O. J. 2022. Experimental study on the properties of sawdust concrete with partial replacement of cement with sawdust ash. Journal of Inventive Engineering and Technology 2.2: 1–11.

Waswa-Sabuni, B., Syagga, P. M., Dulo, S. O. and Kamau, G. N. 2002. Rice husk ash cement – an alternative pozzolana cement for Kenyan building industry. Journal of Civil Engineering, JKUAT 8: 13–26.

WBCSD Cement Sustainability Initiative. 2018. Getting the numbers right (GNR) project reporting. Research 28.10: 1445–1452.